Original Article

Choline suppresses hepatocellular carcinoma progression by attenuating AMPK/mTOR-mediated autophagy via choline transporter SLC5A7 activation

Chen Wang[1#], Zhao-Yan Liu[1,2#], Wen-Ge Huang[3#], Zhi-Jun Yang[1], Qiu-Ye Lan[1,2], Ai-Ping Fang[1,2], Meng-Jun Hou[4], Xiao-Lin Luo[4], Yao-Jun Zhang[5], Si Chen[1,2], Hui-Lian Zhu[1,2]

[1]Department of Nutrition, School of Public Health, Sun Yat-sen University, Guangzhou, China; [2]Guangdong Provincial Key Laboratory of Food, Nutrition and Health, School of Public Health, Sun Yat-sen University, Guangzhou, China; [3]Center of Experimental Animals, Sun Yat-sen University, Guangzhou, China; [4]Experimental and Teaching Center for Public Health, School of Public Health, Sun Yat-sen University, Guangzhou, China; [5]Department of Hepatobiliary Oncology, Sun Yat-sen University Cancer Center, Guangzhou, China

Contributions: (I) Conception and design: HL Zhu, YJ Zhang, S Chen; (II) Administrative support: HL Zhu, YJ Zhang, S Chen, WG Huang; (III) Provision of study materials or patients: HL Zhu, YJ Zhang, S Chen; (IV) Collection and assembly of data: C Wang, ZY Liu, WG Huang, ZJ Yang, QY Lan, AP Fang, MJ Hou, XL Luo; (V) Data analysis and interpretation: C Wang, ZY Liu, WG Huang; (VI) Manuscript writing: All authors; (VII) Final approval of manuscript: All authors.

[#]These authors contributed equally to this work.

Correspondence to: Yao-Jun Zhang, MD. Department of Hepatobiliary Oncology, Sun Yat-sen University Cancer Center, 651 Dongfeng Road East, Guangzhou 510060, China. Email: zhangyuj@sysucc.org.cn; Si Chen, MD; Hui-Lian Zhu, MD. Department of Nutrition, School of Public Health, Sun Yat-sen University, 74 Zhong Shan Road 2, Guangzhou, 510080, China; Guangdong Provincial Key Laboratory of Food, Nutrition and Health, School of Public Health, Sun Yat-sen University, Guangzhou, China. Email: chens59@mail.sysu.edu.cn; zhuhl@mail.sysu.edu.cn.

Background: Hepatocellular carcinoma (HCC) is one of the leading causes of cancer-associated death. Emerging evidence suggests that autophagy plays a critical role in HCC tumorigenesis, metastasis, and prognosis. Choline is an essential nutrient related to prolonged survival and reduced risk of HCC. However, it remains unclear whether this phenomenon is mediated by autophagy.

Methods: Two HCC cell lines (HUH-7 and Hep3B) were used in the present study. Cell growth was evaluated by cell counting kit 8 (CCK-8), colony formation, and *in vivo* mouse xenografts assays. Cell motility was calculated by wound healing and transwell assays. Autophagosomes were measured by transmission electron microscope (TEM), and autophagy flux was detected by mRFP-GFP-labeled LC3 protein. The mRNA level of genes was measured by quantitative real-time PCR (qRT-PCR). The protein levels were detected by Western blotting (WB).Results: We found that choline inhibited the proliferation, migration, and invasion of HCC cells by downregulating autophagy *in vitro* and *in vivo*. Upregulated expression of the solute carrier family 5 member 7 (SLC5A7), a specific choline transporter, correlated with better HCC prognosis. We further discovered that choline could promote SLC5A7 expression, upregulate cytoplasm p53 expression to impair the AMPK/mTOR pathway, and attenuate autophagy. Finally, we found that choline acted synergistically with sorafenib to attenuate HCC development *in vitro* and *in vivo*.

Conclusions: Our findings provide novel insights into choline-mediated autophagy in HCC, providing the foothold for its future application in HCC treatment.

Keywords: Hepatocellular carcinoma (HCC); autophagy; choline; solute carrier family 5 member 7 (SLC5A7)

Submitted Oct 10, 2022. Accepted for publication Mar 01, 2023. Published online May 30, 2023.
doi: 10.21037/hbsn-22-476
View this article at: https://dx.doi.org/10.21037/hbsn-22-476

Introduction

Hepatocellular carcinoma (HCC) is the predominant type of primary liver cancer, which ranks fourth in cancer-associated death worldwide (1). The high incidence and mortality of HCC in developed and developing countries due to hepatitis virus infection and unhealthy lifestyles have created a huge socio-economic burden, especially in China (2). Although significant achievements have been made in the diagnosis and treatment of HCC, the prognosis of this patients remains unsatisfactory. Thus, elucidating the tumorigenesis mechanism and finding novel therapeutic strategies has gained significant momentum in recent years.

Autophagy is a highly conserved catabolic progress in eukaryotes essential in promoting HCC progression (3-5). Once exposed to adverse conditions, such as nutrient deprivation and hypoxia, autophagy promotes HCC development, leading to a poor prognosis (3,6). The development of autophagy is controlled by a highly regulated set of events, including aging (7), oxidative stress (8), inflammation (9), nutrient status (10), etc. Interestingly, nutrient supplementation is widely thought to have a promising auxiliary role in cancer treatment (11,12). Therefore, the beneficial effects of nutrient supplementation in preventing HCC progression and improving prognosis by inhibiting autophagy are worth investigating.

As an essential nutrient, choline can yield a protective effect against several tumors (13-15), including HCC. For example, it has been demonstrated that dietary deficiency of choline and methionine could induce HCC in rats (16), while choline supplementation attenuated high-fat-induced HCC in mice (17). In addition, our previous studies demonstrated that increased dietary choline intake and serum choline level were associated with reduced HCC risk and better survival (18,19). Although growing evidence indicates that choline yields a protective effect against HCC, the underlying mechanism remains uninvestigated. Previous studies found that choline and methionine deficiency-induced nonalcoholic steatohepatitis (NASH) and nonalcoholic fatty liver disease (NAFLD) were accompanied by autophagy induction (20-22), indicating the critical role of autophagy in the relationship between choline and liver diseases.

A recent study revealed the downregulation of a choline-specific transporter, a solute carrier family 5 member 7 (SLC5A7), in colorectal cancer (CRC) and reported that choline-induced SLC5A7 expression inhibited CRC progression by stabilizing cytoplasm p53 (23). Although the induction of autophagy by p53, a well-known tumor suppressor, has been extensively documented in the literature, emerging evidence suggests that p53 in the cytoplasm could inhibit autophagy by attenuating the AMPK/mTOR pathway (24,25). Whether choline could ameliorate the malignant progression of HCC by suppressing autophagy via the SLC5A7/p53/AMPK/mTOR pathway remains largely unclear. The current study aimed to illustrate the antitumor effects and the underlying mechanism of choline in HCC progression.

In the present study, we demonstrated the tumor-suppressive effect of choline on HCC cells. We found that choline inhibited HCC progression by attenuating AMPK/mTOR-dependent autophagy via SLC5A7 activation, which could improve the antitumor effect of sorafenib against HCC. These findings provide further insights into the antitumor roles of choline on HCC and broaden the therapeutic horizons for this patient population. We present this article in accordance with the ARRIVE reporting checklist (available at https://hbsn.amegroups.com/article/view/10.21037/hbsn-22-476/rc).

Highlight box

Key findings

- Our study demonstrated that choline inhibited HCC malignant progression by suppressing AMPK/mTOR-mediated autophagy via SLC5A7 upregulation.

What is known and what is new?

- Epidemiological and animal studies have illustrated the antitumor effect of choline against HCC, but the underlying mechanism remains unknown.
- Here, we demonstrated the possible mechanism of choline in inhibiting the malignant progression of HCC.

What is the implication, and what should change now?

- The synergistic antitumor effect of choline and sorafenib provides a novel insight for HCC treatment in the future, which further implicated that nutritional intervention is a better strategy in the clinical treatment of HCC.

Methods

Sample collection

The present study was conducted based on the "Guangdong Liver Cancer Cohort (GLCC)", which was initiated in 2013

at Sun Yat-sen University Cancer Center. The GLCC was registered at clinicaltrials.gov as NCT03297255. Detailed information on GLCC was described previously (26). A total of 74 HCC patients treated with hepatectomy were selected based on the following inclusion criteria: (I) newly diagnosed within 1 month and without any anti-cancer treatment before surgery; (II) HCC tissues and paired non-tumor tissues available. Written informed consent was obtained from each participant. The Ethics Committee of the School of Public Health at Sun Yat-sen University approved the protocol of GLCC. The study was conducted in accordance with the Declaration of Helsinki (as revised in 2013).

Chemicals and reagents

Choline, rapamycin, and sorafenib were purchased from Sigma-Aldrich (St. Louis, MO, USA), Solarbio (Beijing, China), and MedChem Express (Monmouth Jct., NJ, USA), respectively. Primary antibodies of mTOR, p-mTOR, P70S6K, 4EBP1, p-4EBP1, and Goat Anti-Rabbit IgG H&L (Alexa Fluor® 488) were obtained from Abcam (UK). Primary antibodies of ACTB, LC3B, SQSTM1/p62, BECN1, SLC5A7, p53, AMPK, p-AMPK, and p-P70S6K were purchased from Abclonal (Wuhan, China). The HRP anti-rabbit IgG antibody was obtained from Proteintech (Wuhan, China).

Cell culture

The human HCC cell line HUH-7 and Hep3B were purchased from the Nation Collection of Authenticated Cell Cultures of China (Shanghai, China). HUH-7 cells were cultured in Dulbecco's modified eagle medium (DMEM) supplemented with 10% fetal bovine serum (FBS) and 1% antibiotic-antimycotic. Hep3B cells were incubated in Minimum Essential Medium (MEM) containing 10% FBS and 1% antibiotic-antimycotic. Cells were kept at 37 ℃ in a humidified atmosphere with 5% CO_2. Cells were authenticated before use.

Cell transfection

The small interfering RNA targeting SLC5A7, AMPK, and the negative control (NC) were synthesized by GenePharma (Suzhou, China) and transfected into HCC cells according to the manufacturer's instructions. The expression of SLC5A7 and AMPK was measured by Western Blot assay (Figure S1). The details of SLC5A7 and AMPK siRNA are listed in Table S1.

Cell growth assessment

Approximately 4×10^3 cells of both cell lines were seeded into each well, and the cell counting kit 8 (CCK-8) assay was performed to detect cell proliferation. After exposure to the indicated treatments, 10 μL of CCK-8 reagent was dissolved in 90 μL of serum-free medium and added to each well. After 2 h of incubation, the optical density (OD) was measured by a microplate reader at 450 nm.

For the colony formation assay, 400 cells suspended in 3 mL of medium were added to a 12-well plate and subjected to indicated treatments for 14 days. Subsequently, cells were fixed with 4% isopropyl alcohol and stained with crystal violet. Images were captured, and colonies were counted.

Wound healing assay

Cells were diluted in a medium containing 10% FBS at the density of 5×10^5/mL and plated into a six-well plate. After cells reached 90–95% confluence, five straight scratches were made by a 200 μL sterilized pipette and washed with PBS three times. Images were captured after 0 and 48 h at the same position. The scratch area was measured using ImageJ software, and the relative migration rate was calculated with the following formula: migration rate = $(\text{area}^{0\ h} - \text{area}^{48\ h})/\text{area}^{0\ h}\times100\%$.

Transwell invasion assay

Briefly, 50 μL of Matrigel was pre-coated for 4 h at 37 ℃. Then, 500 μL of medium containing 10% FBS was added into the lower chamber, and approximately 5,000 cells diluted in 100 μL of serum-free medium with indicated treatment were planted into the upper chamber. After incubation for 24 h, cells on the upper chamber without invasion were removed gently with a cotton swab. Cells in the lower chamber were fixed with 4% paraformaldehyde and stained with 0.1% crystal violet. After washing and air-drying, images were captured by a light microscope and the number of invaded migrated cells was measured by ImageJ software.

RNA extraction and quantification

Total RNA from cells and tissues was extracted by the

TransZOL reagent. Then, RNA was quantified, and 500 ng of RNA was used for cDNA synthesis using TransScript® II One-Step gDNA Removal and cDNA Synthesis SuperMix kit according to manufacturers' instructions. Subsequently, quantitative real-time PCR (qRT-PCR) was conducted using TransStart Top Green qPCR SuperMix Kit following the manufacturer's guidelines. The expression of SLC5A7 was normalized to 18S rRNA and calculated according to the $2^{-\Delta\Delta CT}$ method. The details of primers are listed in Table S2.

Western blotting (WB) assay

Proteins were isolated from cells and tissues by radioimmunoprecipitation assay (RIPA) lysis buffer and quantified by the bicinchoninic acid (BCA) method. Approximately 20–30 μg of protein samples were loaded and separated by sodium dodecyl sulphate-polyacrylamide gel electrophoresis (SDS-PAGE). Then, proteins were transferred to polyvinylidene fluoride (PVDF) membranes and blocked in 5% skim milk. Subsequently, membranes were washed and incubated with primary antibodies at 4 ℃ overnight. Afterward, membranes were incubated with a secondary antibody. Finally, membranes were washed and detected by enhanced chemiluminescence, and protein expression was analyzed by ImageJ software. Beta-actin (ACTB) was used as a loading control.

The isolation of proteins from the cytoplasm and nucleus was conducted using a Nuclear and Cytoplasmic Protein Extraction kit (Beyotime, Shanghai, China) according to the manufacturer's instructions. After extraction, proteins were quantified by the BCA method and detected by the WB assay as described above.

Autophagy flux assessment

HUH-7 and Hep3B cells were grown in a six-well plate to detect autophagy flux and reached 40–50% confluence, then were subjected to Ad-mCherry-GFP-LC3B transfection according to the manufacturer's instructions. Then, infected cells were seeded on a confocal petri dish for choline treatment. Finally, the mCherry and GFP labeled LC3B protein was detected through a laser scanning confocal microscope and analyzed by ImageJ software.

Transmission electron microscope (TEM) detection

A TEM was used to detect autophagosomes in HCC cells. After being harvested, cells were quickly fixed with 2.5% glutaraldehyde and stained with phosphotungstic acid. Then, autophagosomes were observed and captured by TEM (JEOL Ltd., Tokyo, Japan, JEM-1230).

Mice models

Four-week-old male BALB/c nude mice (n=5 per group) were obtained from the Laboratory Animal Center of Sun Yat-sen University and bred in the SPF animal facility of the Laboratory Animal Center of Sun Yat-sen University in individually ventilated cages. Animal studies were approved by the animal experiments ethics committee of Sun Yat-sen University (No. 2019-020), in compliance with institutional guidelines for the care and use of animals.

About 5×10^6 HUH-7 cells suspended in a 100 μL mixture (50 μL of serum-free medium with 50 μL of Matrigel) were inoculated into the axilla of mice. After one day of inoculation, mice were weighed and randomly subjected to different treatments: Control group, Choline group (0.32 mg/mL of choline dissolved in drinking water), Choline+Rapa group (0.32 mg/mL of choline dissolved in drinking water, and 2 mg/kg of rapamycin intraperitoneal injected every two days); Sora group (50 mg/kg sorafenib intragastric administrated every two days); Choline+Sora group (0.32 mg/mL of choline dissolved in drinking water, and 50 mg/kg sorafenib intragastric administrated every two days). The concentration of choline used in mice experiments was based on the recommended dosage of choline for humans (male) (550 mg/day). Tumor volume was measured every two days and was calculated with the following formula: $V = (L \times W^2) \times \pi/6$ (V = volume, L = length, and W = width). After 21 days of transplantation, the xenograft tumors were excised, weighed, and kept for the following assays.

Bioinformatic analysis

Bioinformatic analysis of SLC5A7 was carried out using online Kaplan-Meier (KM) Plotter, TNMplot and Shiny Gene Expression Omnibus (GEO) tools as previously described (27-29).

Statistical analysis

All experiments were performed in triplicate, and data were presented as mean ± SD. SPSS 22.0 (IBM, Armonk, NY, USA) and GraphPad Prism 8.0 software were used to

calculate the difference by the Student's *t*-test. A P value <0.05 was statistically significant.

Results

Choline inhibits HCC progression

To investigate whether choline exhibits tumor-suppressive roles against HCC, the CCK-8 assay was conducted to evaluate the cell viability in response to choline treatment in two HCC cell lines (HUH-7 and Hep3B). Choline treatment exerted an inhibitory effect on cell viability in a dose-dependent manner (*Figure 1A*), with an IC50 value of 26.45 and 23.29 μM against HUH-7 and Hep3B cells, respectively, *in vitro* (*Figure 1B*). Accordingly, 20 μM choline was used in the following assays. As expected, 20 μM of choline yielded an inhibitory effect on cell viability of HCC in a time-dependent manner (*Figure 1C*). Moreover, the colony formation assay showed a long-term inhibitory effect of choline on HCC cell proliferation (*Figure 1D*). Then, the influence of choline on the migration and invasion of HCC cells was measured. After exposure to choline, the migration and invasion ability of HCC cells significantly decreased with reduced migration distance and invaded cell abundance (*Figure 1E,1F*).

To further validate the antitumor effects of choline against HCC *in vivo*, a subcutaneous mouse xenograft model was established. Choline yielded a significant inhibitory effect on tumor growth, accompanied by slower tumor volume increase and lighter tumor weight but did not affect mice weight (*Figure 1G-1J*). Besides, we also found that Ki-67 and MMP2 expression was attenuated in choline-treated cells and tumor tissues (*Figure 1K*). Taken together, these findings indicate that choline inhibits HCC development both *in vitro* and *in vivo*.

Choline suppresses autophagy in HCC cells

To assess the alterations in autophagy in response to choline treatment in HCC cells, we quantified the autophagy-associated protein markers, autophagosome, and autophagic flux. Compared with cells in the control group, choline treatment reduced the expression of LC3 II and BECN1 while increasing SQSTM1/p62, indicating the inhibition of autophagy in HCC cells (*Figure 2A*). Consistently, choline-treated mouse xenograft tissues exhibited decreased LC3 II and BECN1 and increased SQSTM1/p62 expression (*Figure 2A*). Meanwhile, starvation-induced (EBSS-treated) autophagy was repressed in HCC cells by choline treatment (*Figure 2B*). Then, we measured the number of autophagosomes under TEM. After choline treatment, a marked reduction in autophagosome abundance was observed (*Figure 2C*). Since the whole process of autophagy could be evaluated by autophagic flux, we transfected HCC cells with mCherry-GFP-LC3 to explore the effect of choline on autophagy flux. It has been reported that mCherry-LC3 (Red puncta) and GFP-LC3 (Green puncta) coexist (Yellow puncta) in autophagosomes while GFP-LC3 is hydrolyzed due to the acidic environment in lysosome after the fusion of autophagosome and lysosome. Thus, the number of red puncta number and yellow puncta reflects autophagy flux activation (30). Compared with cells in the control group, a significant reduction in yellow and red puncta abundance was observed, suggesting inhibition of autophagic flux (*Figure 2D*). Thus, our results illustrate that choline could inhibit autophagy activation in HCC cells.

Choline-mediated autophagy inhibition impairs HCC progression

Subsequently, we investigated whether choline-mediated autophagy inhibition prevents HCC progression. We used rapamycin to activate autophagy in HCC cells. Our results revealed that rapamycin cotreatment significantly reversed the inhibitory effect of choline on autophagy in HCC cells, as evidenced by upregulated LC3 II expression, the increased autophagosome, and yellow and red puncta abundance (*Figure 3A-3C*). Following the restoration of autophagy, the growth of HCC cells was significantly increased in the rapamycin-cotreated group compared with the control group in response to choline treatment (*Figure 3D,3E*). Meanwhile, the induction of autophagy by rapamycin efficiently mitigated choline-induced migration and invasion inhibition (*Figure 3F,3G*). Similar results were obtained concerning HCC cell growth *in vivo*, reversed by autophagy induction but without changes in mouse weight (*Figure 3H-3K*). What's more, the downregulated Ki-67 and MMP2 levels were also restored by autophagy induction *in vitro* and *in vivo* (*Figure 3L,3M*). Collectively, these results implied that choline inhibited HCC progression by attenuating autophagy.

SLC5A7 is involved in the inhibition of autophagy by choline in HCC cells

SLC5A7 is a choline transporter that has been reported to

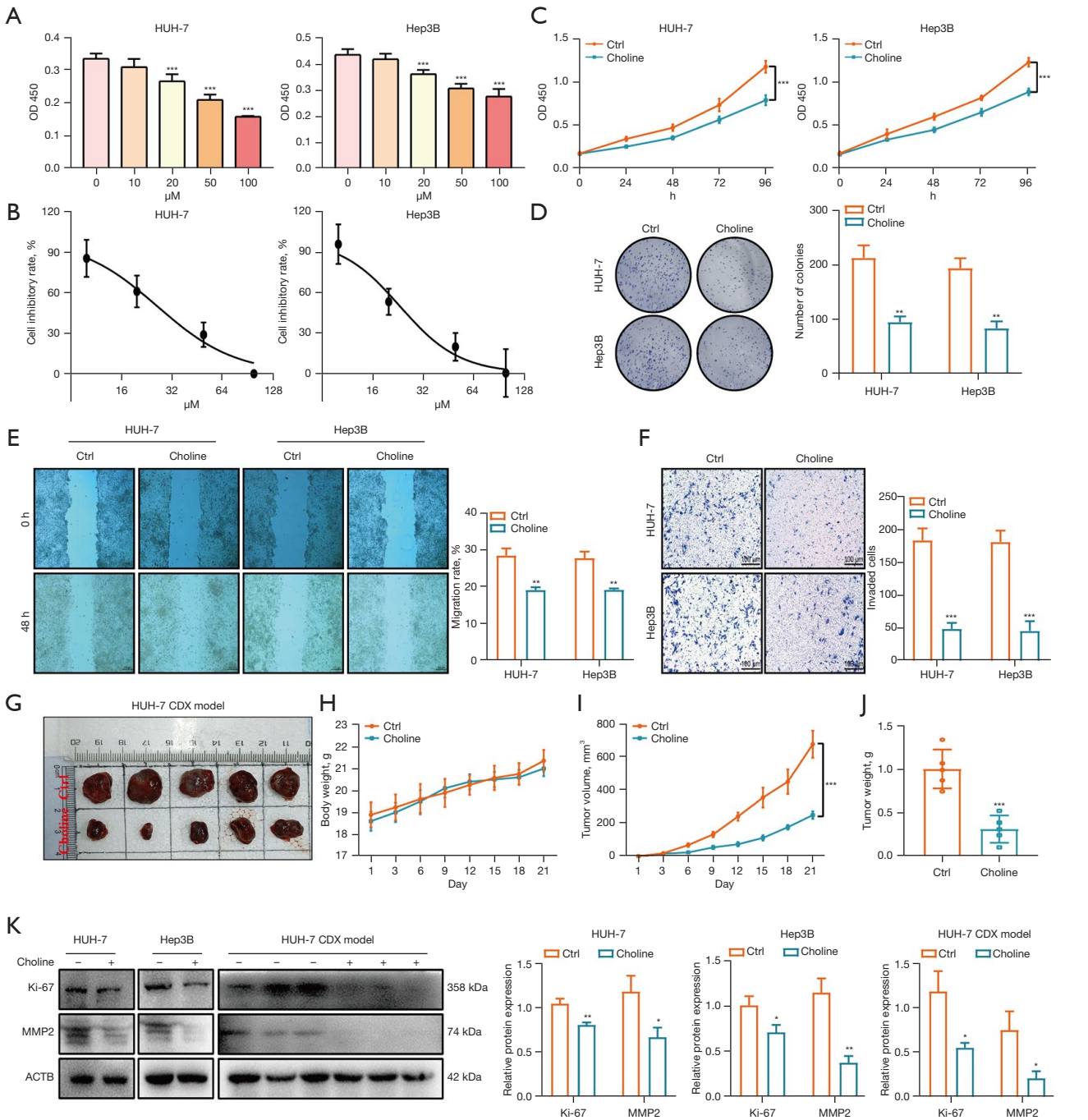

Figure 1 Choline inhibits HCC development *in vitro* and *in vivo*. (A) HUH-7 and Hep3B cells were treated with different choline concentrations for 24 h, and cell viability was detected by CCK-8 assay. (B) Dose-dependent inhibitory curve of choline against HUH-7 and Hep3B cells. (C) HUH-7 and Hep3B cells were subjected to 20 μM of choline, and cell viability was detected every 24 h by CCK-8 assay. (D-F) The effects of choline on HCC cell colony formation, migration, and invasion were measured by colony formation, wound healing, and transwell assays, respectively. Cells in colony formation and transwell assays were stained by 0.1% crystal violet. Scale bar =100 μm. (G-J) Choline inhibited the growth of HUH-7 xenograft tumors (n=5). Tumor volume and mice body weight were measured every two days, and tumor weight was recorded after sacrificing. (K) The level of proteins (Ki-67 and MMP2) in the control and choline groups was analyzed by WB assay, quantified by optical density and normalized to ACTB levels of the same lane. *, choline group *vs.* control group, *, P<0.05; **, P<0.01; ***, P<0.001. OD, optical density; CCK-8, cell counting kit 8; HCC, hepatocellular carcinoma; WB, Western blotting; ACTB, beta-actin.

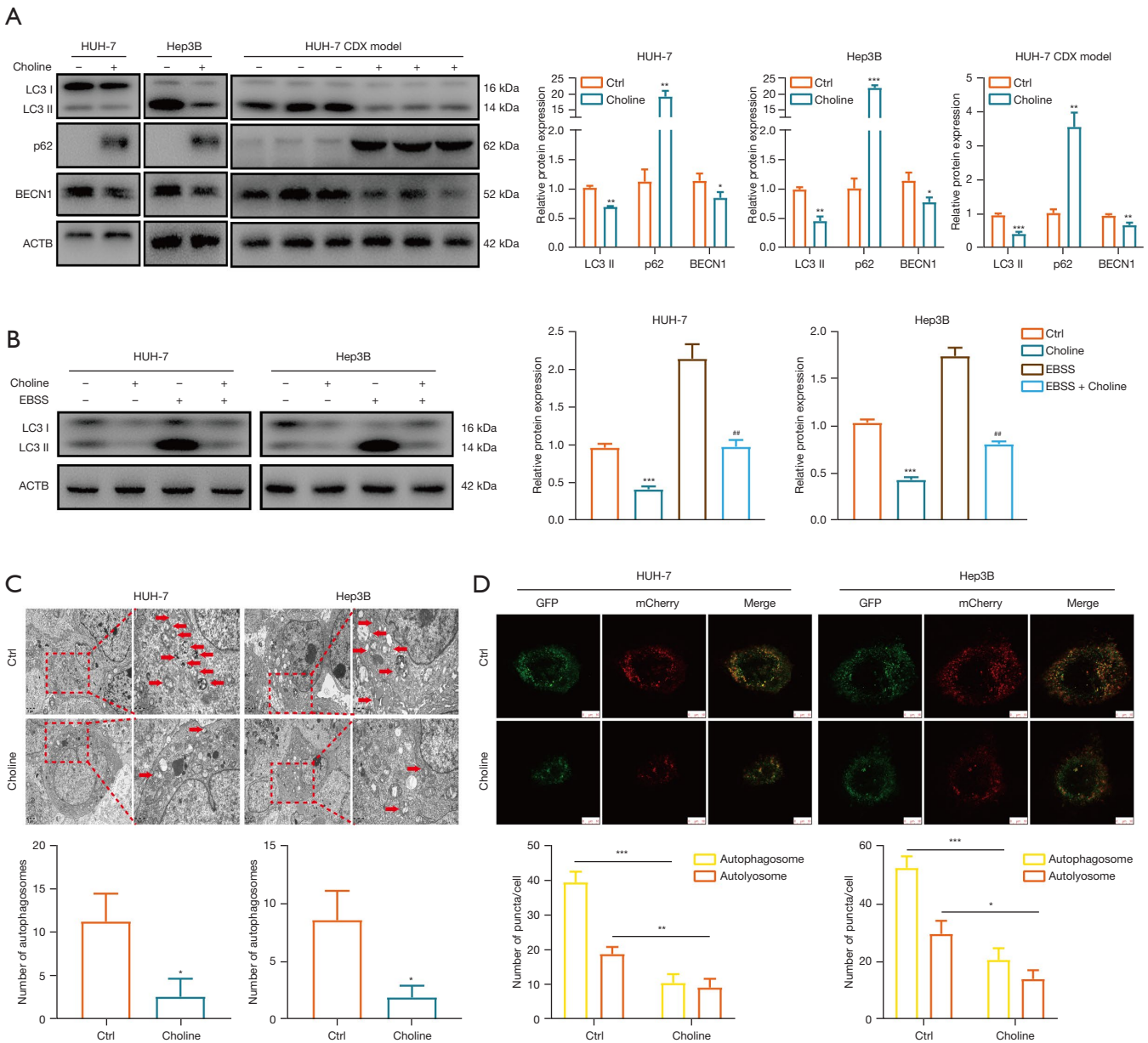

Figure 2 Choline attenuates autophagy activation. (A) WB assay was used to measure the effect of choline on the expression of autophagy-related markers LC3 II, p62, and BECN1, quantitated by optical density and normalized to ACTB levels of the same lane. (B) WB assay was used to detect the effect of choline on starvation-induced autophagy in HCC cells. The expression of LC3 II was quantitated and normalized to ACTB levels of the same lane. (C) Representative images of autophagosomes (red arrows) in HCC cells in response to choline treatment captured by TEM (magnification: left picture =8,000×, right picture =20,000×). (D) mCherry-GFP-LC3 was transfected to HUH-7 and Hep3B cells to detect the influence of choline on autophagy flux. The red puncta represented the autophagolysosomes, and the green puncta represented the autophagosomes. Scale bar =10 μm. *, choline group *vs.* control group; #, EBSS+choline group *vs.* EBSS group, *, P<0.05; **, P<0.01; ***, P<0.001; ##, P<0.01. EBSS, Earle's balanced salt solution; GFP, green fluorescent protein; WB, Western blotting; ACTB, beta-actin; HCC, hepatocellular carcinoma; TEM, transmission electron microscope.

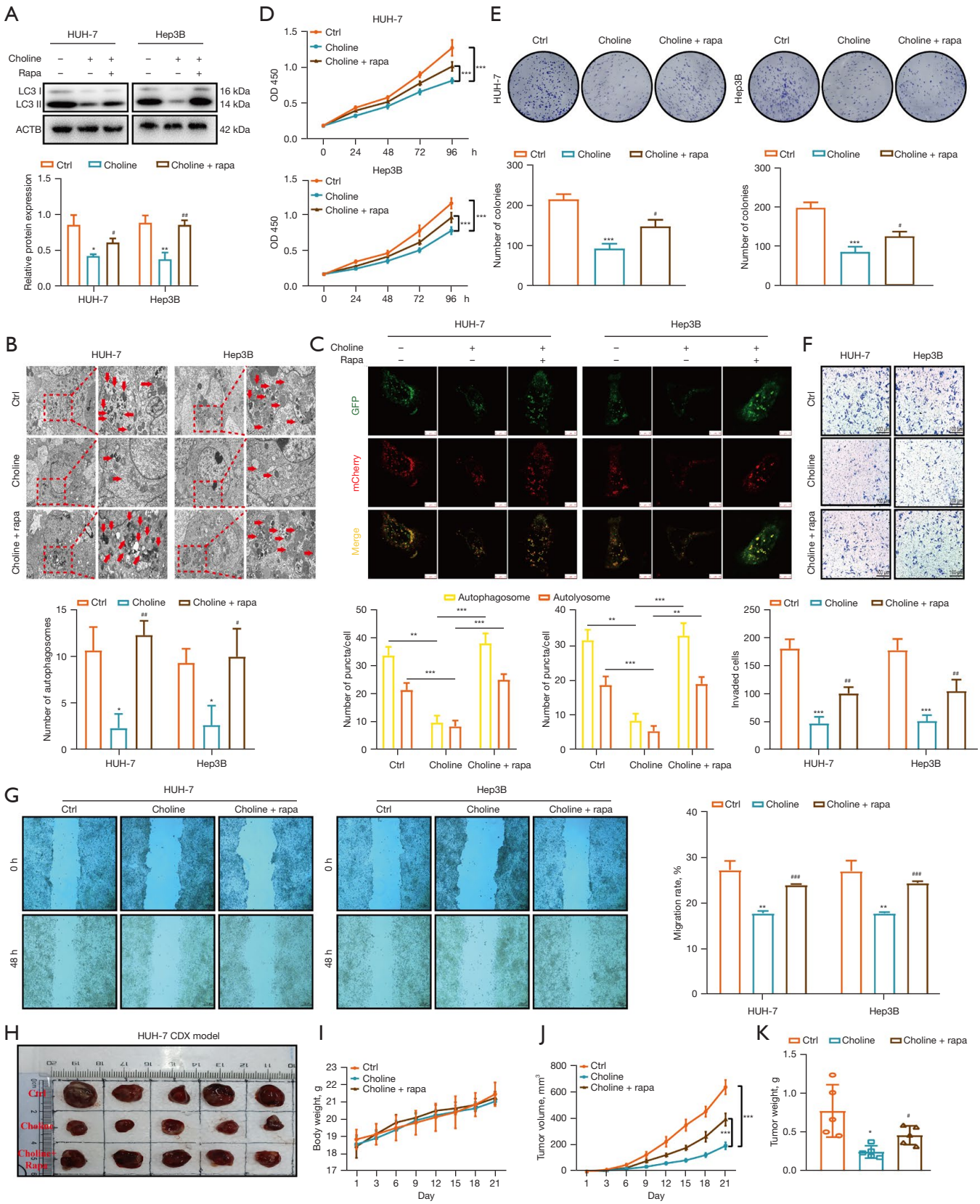

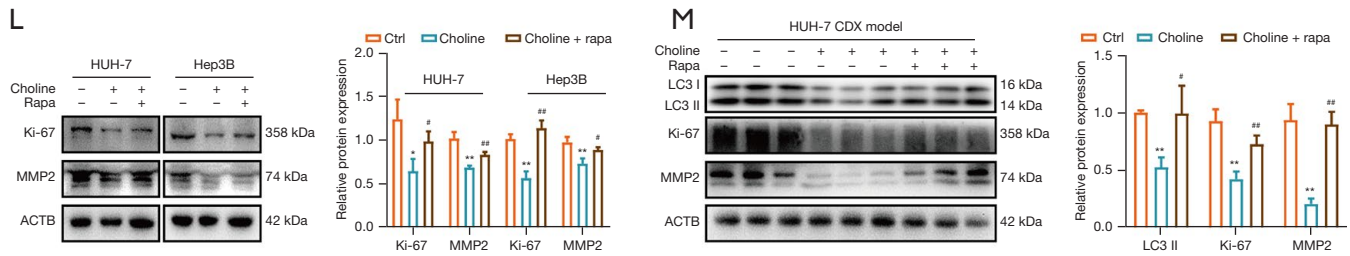

Figure 3 Autophagy induction impairs the tumor suppressive roles of choline on HCC cells. (A) WB analysis of LC3 in HUH-7 and Hep3B cells with choline alone and choline combined with rapamycin. Expression of LC3 II was quantitated based on optical density and normalized to ACTB levels of the same lane. (B) Representative images of autophagosomes (red arrows) in HUH-7 and Hep3B cells treated with choline alone and choline combined with rapamycin were captured with TEM (magnification: left picture =8,000×, right picture =20,000×). (C) mCherry-GFP-LC3 was transfected to HUH-7 and Hep3B cells to detect the influence of choline and choline combined with rapamycin on autophagy flux. The red puncta represented the autophagolysosomes, and the green puncta represented the autophagosomes. Scale bar =10 μm. (D,E) HUH-7 and Hep3B cells were subjected to different treatments in these three groups: control group, choline group, and Choline+Rapa (rapamycin) group. Cell viability was detected by CCK-8 and colony formation assays. Cells in colony formation assay were stained by 0.1% crystal violet. (F,G) Transwell and wound healing assays were used to detect cell migration and invasion under different treatments. Cells in transwell assay were stained by 0.1% crystal violet. Scale bar =100 μm. (H-K) Rapamycin reversed the suppressive role of choline on the growth of HUH-7 xenograft tumors (n=5). Tumor volume and mice body weight were measured every two days, and tumor weight was recorded after sacrificing. (L,M) WB analysis of Ki-67 and MMP2 in HCC cells and HUH-7 xenograft tissues with choline alone and combined with rapamycin treatment. Expression of Ki-67 and MMP2 was quantitated based on optical density and normalized to ACTB levels of the same lane. *, choline group *vs.* control group; $^{\#}$, Choline+Rapa group *vs.* choline group; *, P<0.05; **, P<0.01; ***, P<0.001; $^{\#}$, P<0.05; $^{\#\#}$, P<0.01; $^{\#\#\#}$, P<0.001. ACTB, beta-actin; OD, optical density; GFP, green fluorescent protein; HCC, hepatocellular carcinoma; WB, Western blotting; TEM, transmission electron microscope; CCK-8, cell counting kit 8.

exert antitumor effects on CRC by reducing the degradation of cytoplasmic p53. Interestingly, the results of our in-silico analysis based on GEO data and our cohort study suggested that SLC5A7 was significantly downregulated in HCC tissues compared with non-tumor tissues (*Figure 4A-4C*). Higher expression of SLC5A7 correlated with longer survival and fewer tumor number (*Figure 4D,4E*, and *Table 1*). Correlation analysis also revealed that SLC5A7 was negatively correlated with autophagy markers (*Figure 4F*). We found that choline treatment significantly upregulated SLC5A7 in HCC cells and xenograft tissues as compared with the control group (*Figure 4G,4H*). Silencing of SLC5A7 significantly mitigated the antitumor effect of choline on HCC cells, with accelerated cell viability, increased migration, and invasion (Figure S2A-S2F).

After establishing that choline inhibited autophagy while activating SLC5A7 in HCC cells and a negative correlation was found between SLC5A7 level and autophagy, we investigated whether choline could inhibit autophagy through SLC5A7 stimulation. Results indicated that SLC5A7 silencing significantly restored autophagy inhibited by choline in HCC cells, as illustrated by upregulated LC3 II expression, increased autophagosome and yellow and red puncta abundance (*Figure 4I-4K*), indicating that choline inhibited autophagy by SLC5A7 activation.

Choline inhibits autophagy through SLC5A7/AMPK/mTOR pathway

It has been reported that choline-induced SLC5A7 activation stabilizes cytoplasm p53 in CRC cells, and cytoplasm p53 inhibits autophagy by attenuating the AMPK/mTOR pathway (23,31). Therefore, we explored whether choline inhibited autophagy through SLC5A7-mediated AMPK/mTOR inhibition. First, we found that the expression of total and cytoplasm p53 was upregulated significantly in HCC cells and xenograft tissues in response to choline treatment (*Figure 5A*). Meanwhile, the silencing of SLC5A7 attenuated cytoplasm p53 expression (*Figure 5B*). Next, we assessed the alterations in the AMPK/mTOR pathway in response to choline treatment. Our results indicated that choline treatment significantly inhibited the AMPK/mTOR pathway as demonstrated by decreased p-AMPK level, elevated p-mTOR, p-P70S6K, and p-4EBP1 levels (*Figure 5C,5D*), while silencing of SLC5A7 significantly impaired the inhibition of choline on the

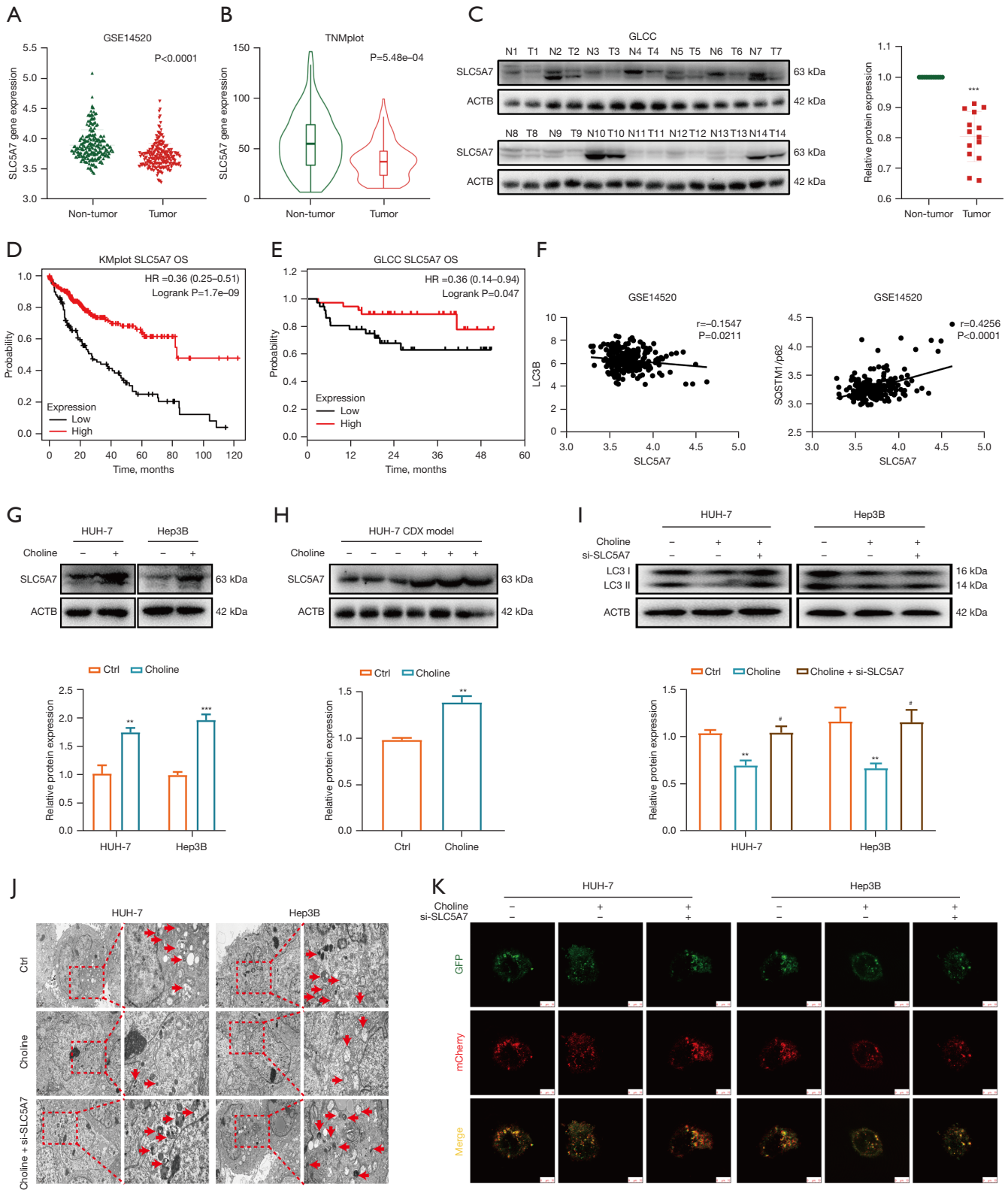

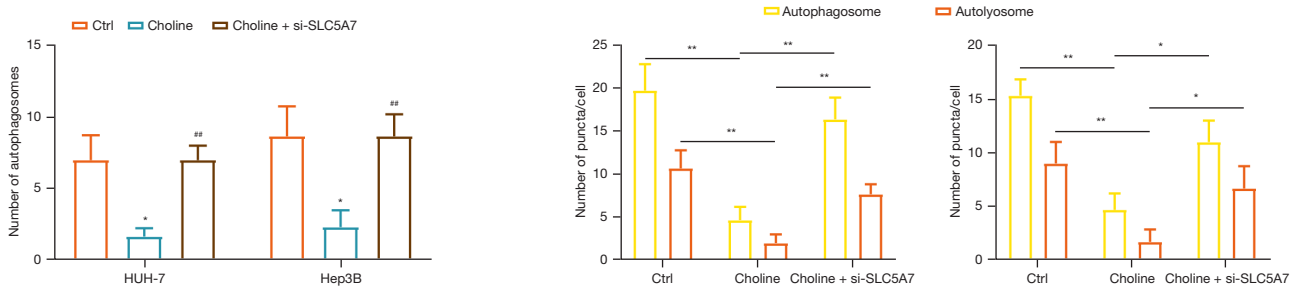

Figure 4 Choline triggers anti-tumor effect by stimulating SLC5A7. (A,B) The expression of SLC5A7 in tumor and paired non-tumor tissues of HCC patients was analyzed by ShinyGEO (GSE14520) and TNMplot. (C) The proteins from 14 paired HCC tumor, and non-tumor tissues were extracted for WB detection. The level of SLC5A7 was measured by optical density and normalized to ACTB levels of the same lane. (D) Overall survival curves for HCC patients stratified by high and low expression of SLC5A7 were analyzed by the online KMplotter tool. (E) Overall survival curves for 74 HCC patients in GLCC stratified by high and low expression of SLC5A7. (F) The correlation of SLC5A7 level with LC3B and p62 expression in HCC using microarray data of GSE14520. (G,H) WB analysis of SLC5A7 in HCC cells and HUH-7 xenograft tissues with choline treatment. Expression of SLC5A7 was normalized to ACTB levels of the same lane. (I) WB analysis of LC3 in HCC cells treated with choline alone and choline combined with si-SLC5A7. Expression of LC3 was quantitated based on optical density. The level of LC3 was normalized to ACTB levels of the same lane. (J) Representative images of autophagosomes (red arrows) in HUH-7 and Hep3B cells treated with choline alone and combined with si-SLC5A7 were captured with TEM (magnification: left picture =8,000×, right picture =20,000×). (K) mCherry-GFP-LC3 was transfected to HUH-7 and Hep3B cells to detect the influence of choline and choline combined with si-SLC5A7 on autophagy flux. The red puncta represented the autophagolysosomes, and the green puncta represented the autophagosomes. Scale bar =10 μm. *, choline group *vs.* control group; #, choline+si-SLC5A7 group *vs.* choline group; *, P<0.05; **, P<0.01; ***, P<0.001; #, P<0.05; ##, P<0.01. TNM, tumor node metastasis; GLCC, Guangdong Liver Cancer Cohort; KM, Kaplan-Meier; HR, hazard ratio; GFP, green fluorescent protein; HCC, hepatocellular carcinoma; WB, Western blotting; ACTB, beta-actin; TEM, transmission electron microscope.

AMPK/mTOR pathway (*Figure 5E*). To confirm that choline-SLC5A7 mediated autophagy inhibition is AMPK/mTOR dependent, we genetically silenced AMPK in HCC cells by transfecting small interfering RNA that specifically targeting AMPK. As the result revealed, the promoting effect of SLC5A7 silencing on autophagy was reversed by silencing AMPK (*Figure 5F*). Taken together, these data indicated that choline could inhibit AMPK/mTOR-dependent autophagy by SLC5A7 activation.

Choline enhances the anti-tumor effect of sorafenib in HCC

As a first-line drug in HCC clinical treatment, sorafenib can only prolong the life span of HCC patients by approximately 3 months, and drug resistance is one of the important reasons for its limited efficacy (32). An increasing body of evidence suggests that autophagy is pivotal in promoting drug resistance (33,34). Thus, we aimed to explore whether choline supplementation could enhance the response of HCC to sorafenib therapy. We found that sorafenib treatment inhibited HCC malignant progression with decreased proliferation, colony formation, migration, and invasion *in vitro* (*Figure 6A-6D*). Interestingly, the combination of choline with sorafenib yielded a more significant inhibitory effect on HCC (*Figure 6A-6D*).

HUH-7 xenograft models demonstrated the synergistic effects of choline and sorafenib *in vivo*. Xenografts subjected to combined treatment showed reduced growth rate, tumor size, and tumor weight but no changes in mice weight (*Figure 6E-6H*). Further analysis revealed that choline treatment could lead to a 65% reduction in tumor volume and weight (*Figure 1I,1J*, *Figure 3J,3K*). However, additional choline supplementation led to a 72% and 79% reduction in tumor volume and weight, respectively, compared with sorafenib alone (*Figure 6G,6H*). Similarly, combined treatment remarkably suppressed Ki-67 and MMP2 levels *in vitro* and *in vivo* (*Figure 6I,6J*). Taken together, choline could enhance the antitumor effect of sorafenib against HCC.

Discussion

In the present study, we explored the effects and

Table 1 The association between SLC5A7 levels and clinicopathological characteristics of 74 patients with hepatocellular carcinoma

Variables	All cases (n=74)	SLC5A7 expression		P values
		Low (n=38)	High (n=36)	
Age (years)				0.816
≤50	35	17	18	
>50	39	21	18	
Sex				0.339
Male	63	34	29	
Female	11	4	7	
HBsAg				1.000
Negative	9	5	4	
Positive	65	33	32	
Tumor size				0.640
<3 cm	29	16	13	
≥3 cm	45	22	23	
Tumor number				0.005*
≤1	47	24	33	
>1	17	14	3	
TNM stage				0.178
I–II	56	26	30	
III–IV	18	12	6	
Cirrhosis				0.780
No	16	9	7	
Yes	58	29	29	
Recurrence/ metastasis				0.621
No	24	11	13	
Yes	50	27	23	
AFP (ng/mL)				0.476
<40	29	13	16	
≥40	45	25	20	
CEA (ng/mL)				1.000
<5	60	31	29	
≥5	14	7	7	
CA199 (IU/mL)				0.599
<35	55	27	28	
≥35	19	11	8	
CRP (mg/L)				0.578
<8	58	31	27	
≥8	16	7	9	
BCLC				0.077
0–A	52	23	29	
B–C	22	15	7	

*, P<0.05 was considered significant. SLC5A7, solute carrier family 5 member 7; HBsAg, hepatitis B surface antigen; TNM, tumor node metastasis; AFP, alpha-fetoprotein; CEA, carcinoembryonic antigen; CA199, carbohydrate antigen199; CRP, C-reactive protein; BCLC, Barcelona Clinic Liver Cancer Classification.

mechanisms involved in regulating autophagy in response to choline supplementation in HCC cells. Our results indicated that choline inhibits HCC cell progression by suppressing autophagy. Interestingly, we found that choline activates SLC5A7 expression, resulting in cytoplasm p53 upregulation and AMPK/mTOR pathway inhibition. The inhibition of autophagy led to the suppression of HCC cell development. Importantly, the present study provides hitherto undocumented insights into choline-mediated HCC suppression, emphasizing the mechanism of SLC5A7/AMPK/mTOR in autophagy attenuation (*Figure 7*).

Choline is an important nutrient that reportedly protects against several cancers, including HCC (13). *In vivo* mouse experiments showed that a choline-deficient diet could induce HCC initiation without carcinogens (16), while choline supplementation protects high-fat diet-induced HCC (17). In the present study, we provided compelling evidence of the tumor suppressive roles of choline against HCC cells *in vitro* and *in vivo* and investigated the underlying mechanisms. It is well-established that autophagy may maintain cell survival by degrading damaged organelles, misfolded proteins, and other unwanted materials to provide nutrients (30). Autophagy could be either stimulated by a tumor-promoting pathway to potentiate HCC progression or by nutrition deprivation or chemotherapeutic reagent to support cell survival (35). Thus, targeting autophagy attenuation could be used to inhibit HCC malignant progression and improve the efficacy of clinical drugs. It has been reported that

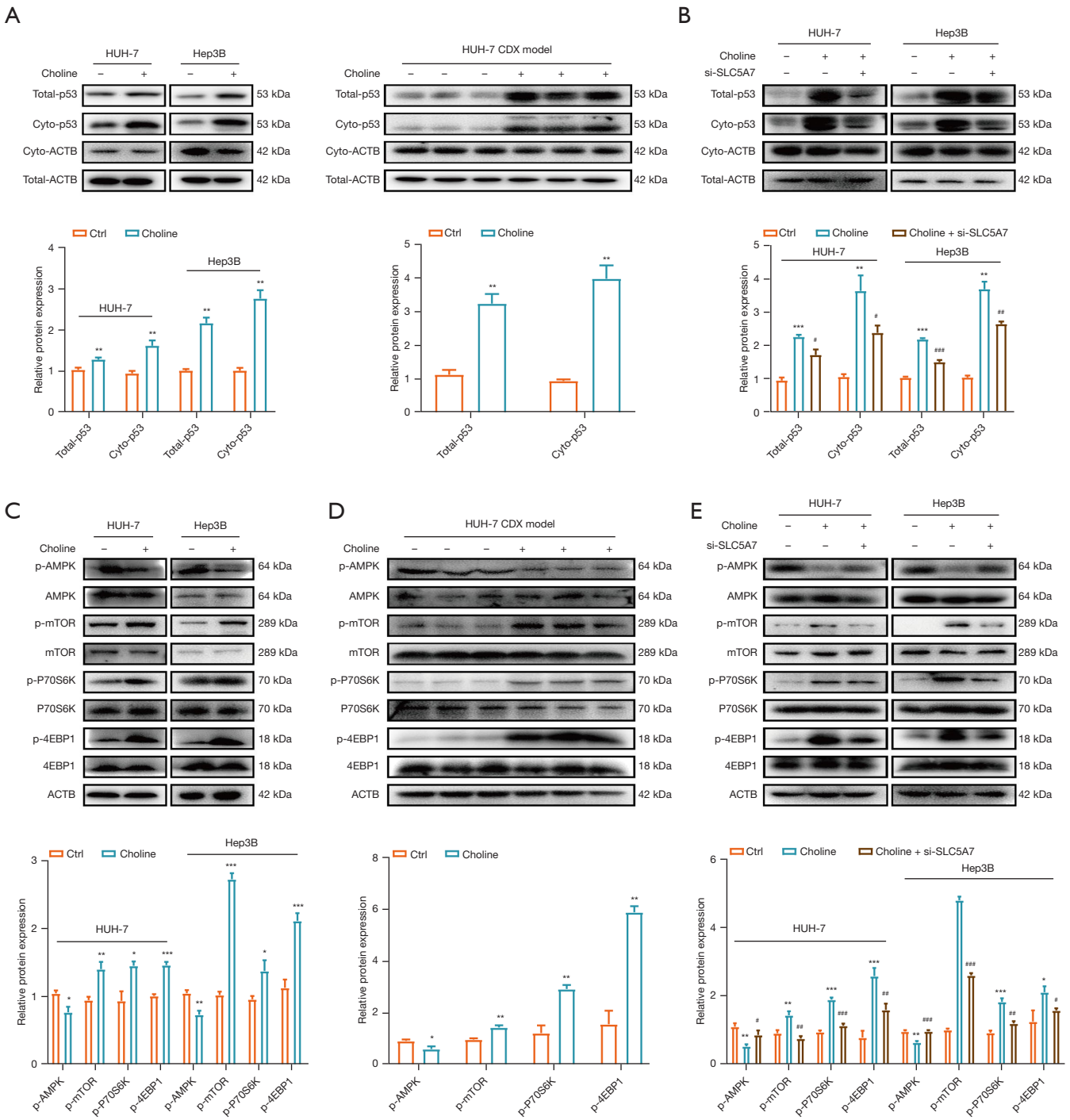

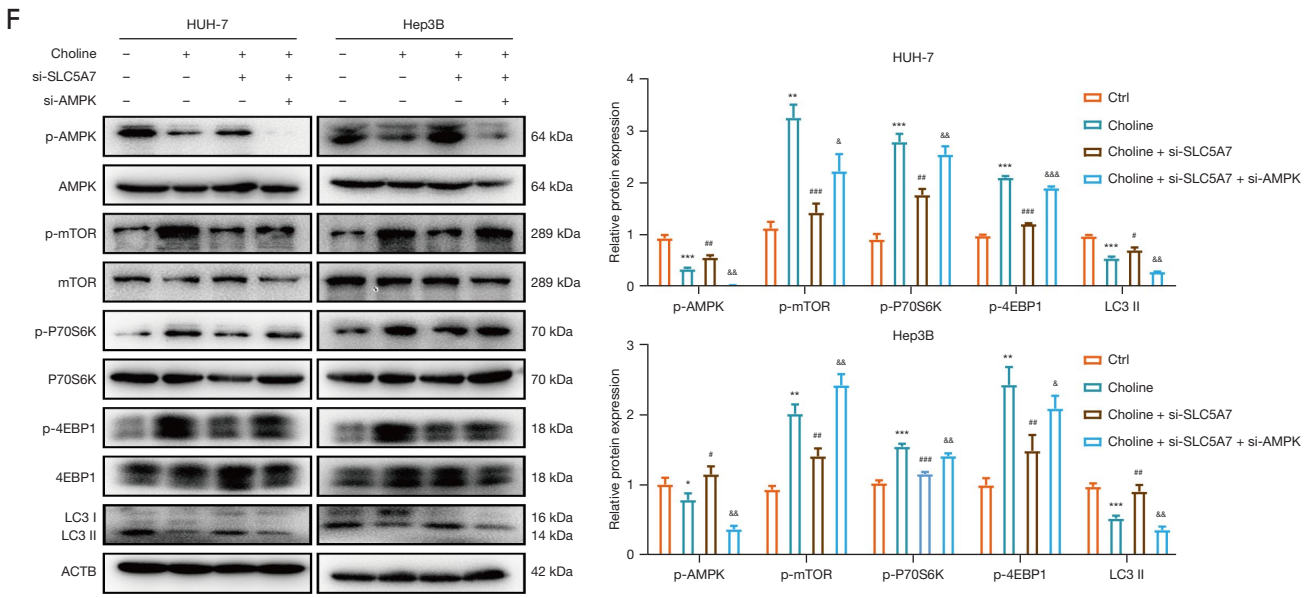

Figure 5 Choline inhibits autophagy through SLC5A7/AMPK/mTOR pathway. (A) WB analysis of total p53 and cytoplasm p53 in HCC cells treated with choline. Expression of total p53 and cytoplasm p53 was quantitated based on optical density. The level of total p53 and cytoplasm p53 was normalized to ACTB levels of the same lane. (B) WB analysis of total p53 and cytoplasm p53 in HCC cells treated with choline alone and combined with si-SLC5A7. Expression of total p53 and cytoplasm p53 was quantitated based on optical density. The level of total p53 and cytoplasm p53 was normalized to ACTB levels of the same lane. (C,D) WB analysis of p-AMPK, total AMPK, p-mTOR, total mTOR, p-P70S6K, total P70S6K, p-4EBP1, and total 4EBP1 in HCC cells and HUH-7 xenograft tissues with choline treatment. Expression of p-AMPK, total AMPK, p-mTOR, total mTOR, p-P70S6K, total P70S6K, p-4EBP1, and total 4EBP1 was quantitated based on optical density and normalized to ACTB levels of the same lane. (E) WB analysis of p-AMPK, total AMPK, p-mTOR, total mTOR, p-P70S6K, total P70S6K, p-4EBP1, and total 4EBP1 in HCC cells with choline alone and choline combined with si-SLC5A7. Expression of p-AMPK, total AMPK, p-mTOR, total mTOR, p-P70S6K, total P70S6K, p-4EBP1, and total 4EBP1, was quantified based on optical density and normalized to ACTB levels of the same lane. (F) HUH-7 and Hep3B cells were subjected to four groups: Control group, Choline group, Choline+si-SLC5A7 group, and Choline+si-SLC5A7+si-AMPK group. WB analysis of p-AMPK, total AMPK, p-mTOR, total mTOR, p-P70S6K, total P70S6K, p-4EBP1, total 4EBP1, and LC3 in HCC cells. Expression of p-AMPK, total AMPK, p-mTOR, total mTOR, p-P70S6K, total P70S6K, p-4EBP1, total 4EBP1, and LC3 was quantitated based on optical density and normalized to ACTB levels of the same lane. *, choline group *vs.* control group; $^{\#}$, choline+si-SLC5A7 group *vs.* choline group; $^{\&}$, choline+si-SLC5A7+si-AMPK group *vs.* choline+si-SLC5A7 group; *, P<0.05; **, P<0.01; ***, P<0.001; $^{\#}$, P<0.05; $^{\#\#}$, P<0.01; $^{\#\#\#}$, P<0.001; $^{\&}$, P<0.05; $^{\&\&}$, P<0.01; $^{\&\&\&}$, P<0.001. ACTB, beta-actin; WB, Western blotting; HCC, hepatocellular carcinoma.

choline-deficient diet-induced NASH and NAFLD were accompanied by autophagy induction, indicating the important role of autophagy in choline-related liver diseases (20-22). Herein, we provided compelling evidence that choline-inhibited autophagy attenuated HCC malignant progression and sensitized HCC cells to sorafenib treatment. In line with our findings, Alhamad *et al.* reported that after spautin-inhibited autophagy, HCC cells were sensitized to fingolimod treatment (36). He *et al.* revealed that zingiberensis newsaponin-impaired autophagy inhibited HCC malignant progression (37). Overall, the above findings suggest that targeting autophagy with nutrients or natural products may inhibit HCC progression and provide a new strategy for HCC treatment.

The solute carrier (SLC) superfamily is vital for transmembrane delivery that consists of 53 families with more than 400 proteins to sustain homeostasis (38). SLC5A7 is the specific transporter of extracellular choline and can be activated by choline stimulus (39). Although its functions in brain-associated diseases have been well investigated, little research has been conducted in tumors (40,41). Recent studies revealed that a high SLC5A7 expression

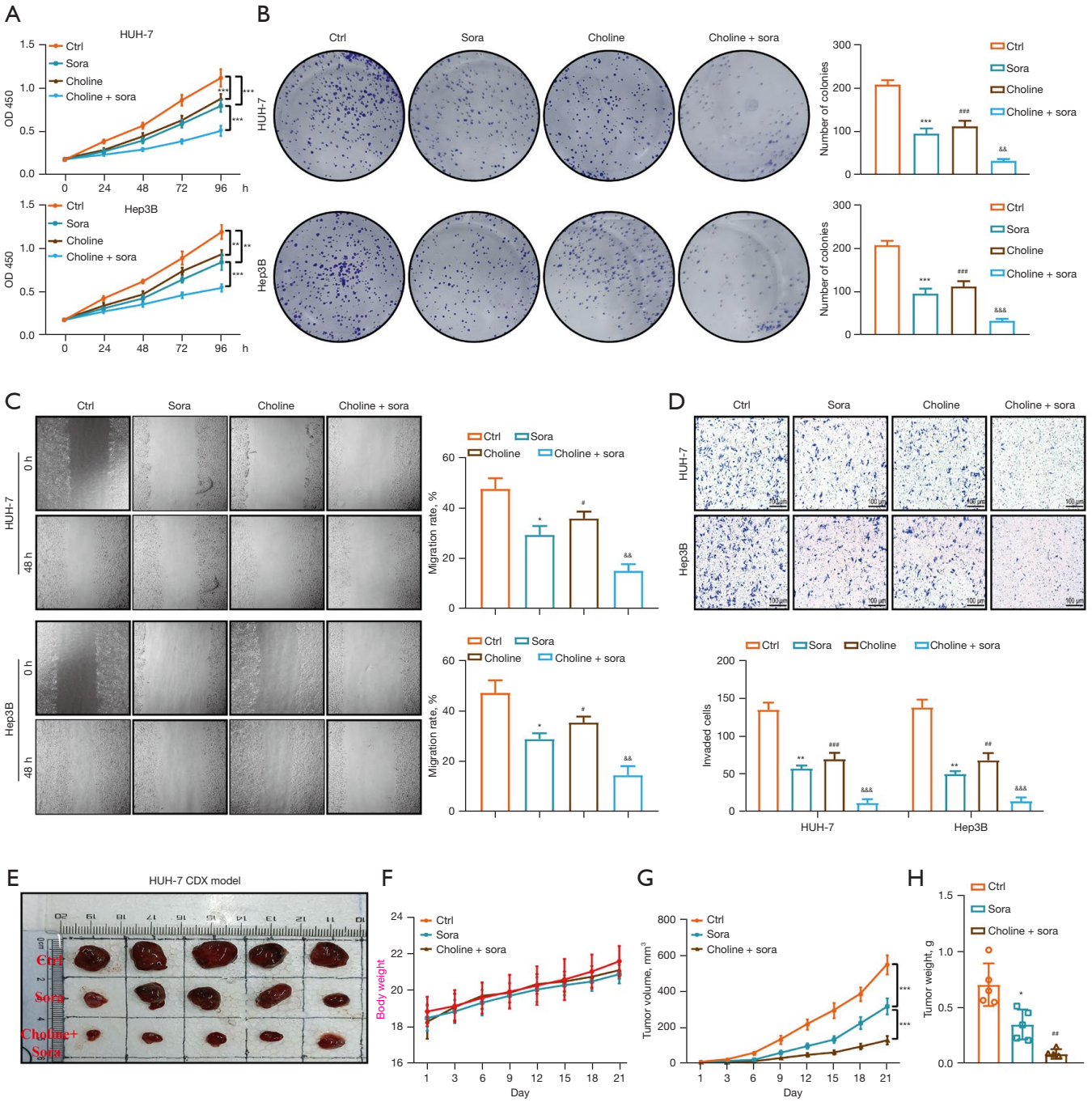

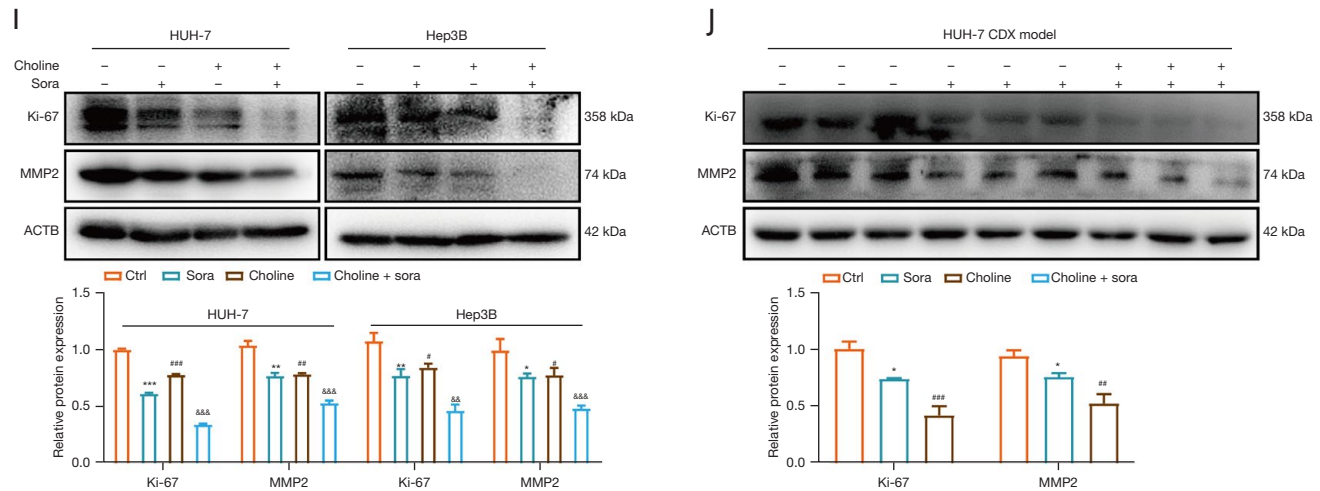

Figure 6 Choline enhances the anti-tumor effects of sorafenib. (A,B) HUH-7 and Hep3B cells were subjected to four groups: control group, Sora (sorafenib) group, choline group and Choline+Sora group. Cell growth was detected by CCK-8 and colony formation assays *in vitro*. Cells in colony formation assay were stained by 0.1% crystal violet. (C,D) Wound healing and transwell assays were used to detect cell migration and invasion under different treatments, respectively. Cells in transwell assay were stained by 0.1% crystal violet. Scale bar =100 μm. (E-H) Choline synergized the antitumor effect of sorafenib in HUH-7 xenograft tumors (n=5). Tumor volume and mice body weight were measured every two days, and tumor weight was recorded after sacrificing. (I,J) WB analysis of Ki-67 and MMP2 in HCC cells and HUH-7 xenograft tissues treated with sorafenib alone or in combination with choline. Expression of Ki-67 and MMP2 was quantitated based on optical density and normalized to ACTB levels of the same lane. *, Sora group *vs.* control group; $^{\#}$, choline group *vs.* control group; $^{\&}$, Choline+Sora group *vs.* Sora group; *, P<0.05; **, P<0.01; ***, P<0.001; $^{\#}$, P<0.05; $^{\#\#}$, P<0.01; $^{\#\#\#}$, P<0.001; $^{\&\&}$, P<0.01; $^{\&\&\&}$, P<0.001. OD, optical density; ACTB, beta-actin; CCK-8, cell counting kit 8; WB, Western blotting; HCC, hepatocellular carcinoma.

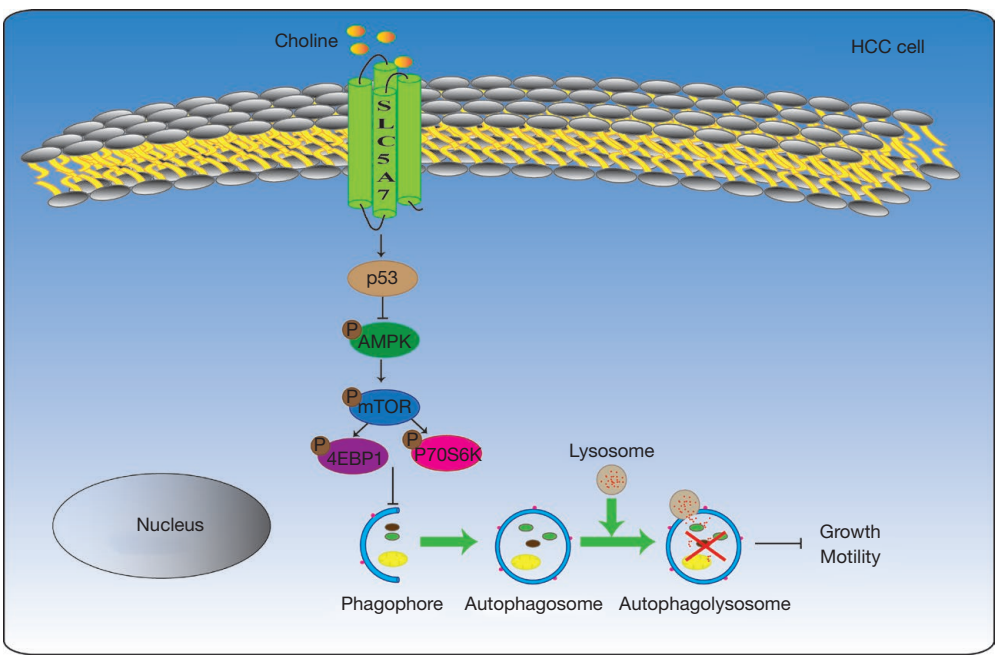

Figure 7 Schematic diagram of the inhibitory effect of choline on HCC progression. HCC, hepatocellular carcinoma.

correlated with better prognosis, and ectopic expression or demethylation of SLC5A7 attenuated cancer cell malignant progression (23,42). Consistently, our results demonstrated that SLC5A7 was downregulated in HCC tissues, and its levels were positively associated with a good prognosis in HCC patients. Besides, we revealed that choline could stimulate SLC5A7 expression in HCC cell lines and xenograft models. Therefore, SLC5A7 may be a candidate target of choline to exert its antitumor effects in HCC.

Our bioinformatic analysis revealed that SLC5A7 levels were negatively correlated with autophagy in HCC tissues. Interestingly, the activation of SLC5A7 by choline treatment plays a pivotal role in mitigating malignant progression and autophagy attenuation in HCC cells. Silencing of SLC5A7 impaired the antitumor effect of choline and prevented choline-mediated autophagy attenuation in HCC cells. These findings corroborate the importance of SLC5A7 in the relationship between choline and autophagy in HCC cells. However, currently little is known about how the transmembrane SLC5A7 mediates autophagy attenuation in response to choline treatment, emphasizing the need for further investigation.

After activation, SLC5A7 directly binds with cytoplasm p53 and disrupts the interaction between cytoplasm p53 and MDM2 to prevent cytoplasm p53 degradation (23). Consistently, our results revealed that choline treatment significantly promoted cytoplasm p53 expression in HCC cells and xenograft tissues, and silencing of SLC5A7 mitigated cytoplasm p53 levels that were initially upregulated by choline. Interestingly, recent study revealed that cytoplasm p53 functions as a negative regulator of autophagy by inhibiting AMPK/mTOR pathway (31). In line with the literature, we demonstrated that choline treatment attenuated the AMPK/mTOR pathway in HCC cells and xenograft models while silencing of SLC5A7 mitigated the effect of choline on the AMPK/mTOR pathway. Furthermore, by silencing AMPK, the mitigation of SLC5A7 silencing on the choline-mediated AMPK/mTOR pathway was partially reversed. These data indicated that choline-induced SLC5A7 inhibited autophagy via AMPK/mTOR pathway.

Conclusions

Taken together, our findings suggest that downregulated autophagy may be the primary contributing factor to prevent HCC malignant progression in response to choline treatment. Meanwhile, SLC5A7-mediated AMPK/mTOR pathway inhibition was responsible for autophagy inhibition. To our knowledge, this is the first study to demonstrate the mechanism underlying the antitumor effect of choline in HCC. Moreover, the synergistic effects of choline and sorafenib may provide a new strategy for HCC treatment.

Acknowledgments

Funding: This work was supported by the Basic and Applied Basic Research Foundation of Guangdong province, China (grant number 2020A1515110682), Guangdong Provincial science and technology project (grant number 2017A040406008), the National Natural Science Foundation of China (grant numbers 81973016, 82103825), the Postdoctoral Science Foundation of China (grant number 2020M683135).

Footnote

Reporting Checklist: The authors have completed the ARRIVE reporting checklist. Available at https://hbsn.amegroups.com/article/view/10.21037/hbsn-22-476/rc

Data Sharing Statement: Available at https://hbsn.amegroups.com/article/view/10.21037/hbsn-22-476/dss

Conflicts of Interest: All authors have completed the ICMJE uniform disclosure form (available at https://hbsn.amegroups.com/article/view/10.21037/hbsn-22-476/coif). The authors have no conflicts of interest to declare.

Ethical Statement: The authors are accountable for all aspects of the work in ensuring that questions related to the accuracy or integrity of any part of the work are appropriately investigated and resolved. The study was conducted in accordance with the Declaration of Helsinki (as revised in 2013). The Ethics Committee of the School of Public Health at Sun Yat-sen University approved the protocol of GLCC. Written informed consent was obtained from each participant. Animal studies were approved by the animal experiments ethics committee of Sun Yat-sen University (No. 2019-020), in compliance with institutional guidelines for the care and use of animals.

References

1. Gordan JD, Kennedy EB, Abou-Alfa GK, et al. Systemic Therapy for Advanced Hepatocellular Carcinoma: ASCO Guideline. J Clin Oncol 2020;38:4317-45.
2. Kulik L, El-Serag HB. Epidemiology and Management of Hepatocellular Carcinoma. Gastroenterology 2019;156:477-491.e1.
3. Li Q, Ni Y, Zhang L, et al. HIF-1α-induced expression of m6A reader YTHDF1 drives hypoxia-induced autophagy and malignancy of hepatocellular carcinoma by promoting ATG2A and ATG14 translation. Signal Transduct Target Ther 2021;6:76.
4. Chen Z, Liu S, Xie P, et al. Tumor-derived PD1 and PD-L1 could promote hepatocellular carcinoma growth through autophagy induction in vitro. Biochem Biophys Res Commun 2022;605:82-9.
5. Zhang X, Bai Y, Huang L, et al. CHD1L augments autophagy-mediated migration of hepatocellular carcinoma through targeting ZKSCAN3. Cell Death Dis 2021;12:950.
6. Song J, Guo X, Xie X, et al. Autophagy in hypoxia protects cancer cells against apoptosis induced by nutrient deprivation through a Beclin1-dependent way in hepatocellular carcinoma. J Cell Biochem 2011;112:3406-20.
7. Rubinsztein DC, Mariño G, Kroemer G. Autophagy and aging. Cell 2011;146:682-95.
8. Filomeni G, De Zio D, Cecconi F. Oxidative stress and autophagy: the clash between damage and metabolic needs. Cell Death Differ 2015;22:377-88.
9. Matsuzawa-Ishimoto Y, Hwang S, Cadwell K. Autophagy and Inflammation. Annu Rev Immunol 2018;36:73-101.
10. Lee JM, Wagner M, Xiao R, et al. Nutrient-sensing nuclear receptors coordinate autophagy. Nature 2014;516:112-5.
11. Anderson PM, Lalla RV. Glutamine for Amelioration of Radiation and Chemotherapy Associated Mucositis during Cancer Therapy. Nutrients 2020;12:1675.
12. Szewczuk M, Gasiorowska E, Matysiak K, et al. The role of artificial nutrition in gynecological cancer therapy. Ginekol Pol 2019;90:167-72.
13. Youn J, Cho E, Lee JE. Association of choline and betaine levels with cancer incidence and survival: A meta-analysis. Clin Nutr 2019;38:100-9.
14. Awwad HM, Geisel J, Obeid R. The role of choline in prostate cancer. Clin Biochem 2012;45:1548-53.
15. Bagnoli M, Granata A, Nicoletti R, et al. Choline Metabolism Alteration: A Focus on Ovarian Cancer. Front Oncol 2016;6:153.
16. Ghoshal AK, Farber E. The induction of liver cancer by dietary deficiency of choline and methionine without added carcinogens. Carcinogenesis 1984;5:1367-70.
17. Brown AL, Conrad K, Allende DS, et al. Dietary Choline Supplementation Attenuates High-Fat-Diet-Induced Hepatocellular Carcinoma in Mice. J Nutr 2020;150:775-83.
18. Liu ZY, Zhang DM, Yishake D, et al. Dietary choline, rather than betaine intake, is associated with hepatocellular carcinoma mortality. Food Funct 2020;11:7866-77.
19. Liu ZY, Yishake D, Fang AP, et al. Serum choline is associated with hepatocellular carcinoma survival: a prospective cohort study. Nutr Metab (Lond) 2020;17:25.
20. Park HS, Song JW, Park JH, et al. TXNIP/VDUP1 attenuates steatohepatitis via autophagy and fatty acid oxidation. Autophagy 2021;17:2549-64.
21. Wang X, de Carvalho Ribeiro M, Iracheta-Vellve A, et al. Macrophage-Specific Hypoxia-Inducible Factor-1α Contributes to Impaired Autophagic Flux in Nonalcoholic Steatohepatitis. Hepatology 2019;69:545-63.
22. Veskovic M, Mladenovic D, Milenkovic M, et al. Betaine modulates oxidative stress, inflammation, apoptosis, autophagy, and Akt/mTOR signaling in methionine-choline deficiency-induced fatty liver disease. Eur J Pharmacol 2019;848:39-48.
23. Yin Y, Jiang Z, Fu J, et al. Choline-induced SLC5A7 impairs colorectal cancer growth by stabilizing p53 protein. Cancer Lett 2022;525:55-66.
24. Zhu J, Ao H, Liu M, et al. UBE2T promotes autophagy via the p53/AMPK/mTOR signaling pathway in lung adenocarcinoma. J Transl Med 2021;19:374.
25. Kim SM, Ha SE, Lee HJ, et al. Sinensetin Induces Autophagic Cell Death through p53-Related AMPK/mTOR Signaling in Hepatocellular Carcinoma HepG2 Cells. Nutrients 2020;12:2462.
26. Fang AP, Long JA, Zhang YJ, et al. Serum Bioavailable, Rather Than Total, 25-hydroxyvitamin D Levels Are Associated With Hepatocellular Carcinoma Survival. Hepatology 2020;72:169-82.

27. Lánczky A, Győrffy B. Web-Based Survival Analysis Tool Tailored for Medical Research (KMplot): Development and Implementation. J Med Internet Res 2021;23:e27633.
28. Bartha Á, Győrffy B. TNMplot.com: A Web Tool for the Comparison of Gene Expression in Normal, Tumor and Metastatic Tissues. Int J Mol Sci 2021.
29. Dumas J, Gargano MA, Dancik GM. shinyGEO: a web-based application for analyzing gene expression omnibus datasets. Bioinformatics 2016;32:3679-81.
30. Klionsky DJ, Abdel-Aziz AK, Abdelfatah S, et al. Guidelines for the use and interpretation of assays for monitoring autophagy (4th edition)(1). Autophagy 2021;17:1-382.
31. Tasdemir E, Maiuri MC, Galluzzi L, et al. Regulation of autophagy by cytoplasmic p53. Nat Cell Biol 2008;10:676-87.
32. Keating GM. Sorafenib: A Review in Hepatocellular Carcinoma. Target Oncol 2017;12:243-53.
33. Zamame Ramirez JA, Romagnoli GG, Kaneno R. Inhibiting autophagy to prevent drug resistance and improve anti-tumor therapy. Life Sci 2021;265:118745.
34. Wu Y, Zhang J, Li Q. Autophagy, an accomplice or antagonist of drug resistance in HCC? Cell Death Dis 2021;12:266.
35. Huang F, Wang BR, Wang YG. Role of autophagy in tumorigenesis, metastasis, targeted therapy and drug resistance of hepatocellular carcinoma. World J Gastroenterol 2018;24:4643-51.
36. Alhamad DW, Elgendy SM, Hersi F, et al. The inhibition of autophagy by spautin boosts the anticancer activity of fingolimod in multidrug-resistant hepatocellular carcinoma. Life Sci 2022;304:120699.
37. He K, Liu X, Cheng S, et al. Zingiberensis Newsaponin Inhibits the Malignant Progression of Hepatocellular Carcinoma via Suppressing Autophagy Moderated by the AKR1C1-Mediated JAK2/STAT3 Pathway. Evid Based Complement Alternat Med 2021;2021:4055209.
38. Pizzagalli MD, Bensimon A, Superti-Furga G. A guide to plasma membrane solute carrier proteins. FEBS J 2021;288:2784-835.
39. Haga T. Molecular properties of the high-affinity choline transporter CHT1. J Biochem 2014;156:181-94.
40. Donovan E, Avila C, Klausner S, et al. Disrupted Choline Clearance and Sustained Acetylcholine Release In Vivo by a Common Choline Transporter Coding Variant Associated with Poor Attentional Control in Humans. J Neurosci 2022;42:3426-44.
41. Rodríguez Cruz PM, Hughes I, Manzur A, et al. Presynaptic congenital myasthenic syndrome due to three novel mutations in SLC5A7 encoding the sodium-dependant high-affinity choline transporter. Neuromuscul Disord 2021;31:21-8.
42. Li Y, Liu B, Yin X, et al. Targeted demethylation of the SLC5A7 promotor inhibits colorectal cancer progression. Clin Epigenetics 2022;14:92.

Cite this article as: Wang C, Liu ZY, Huang WG, Yang ZJ, Lan QY, Fang AP, Hou MJ, Luo XL, Zhang YJ, Chen S, Zhu HL. Choline suppresses hepatocellular carcinoma progression by attenuating AMPK/mTOR-mediated autophagy via choline transporter SLC5A7 activation. Hepatobiliary Surg Nutr 2023. doi: 10.21037/hbsn-22-476

Supplementary

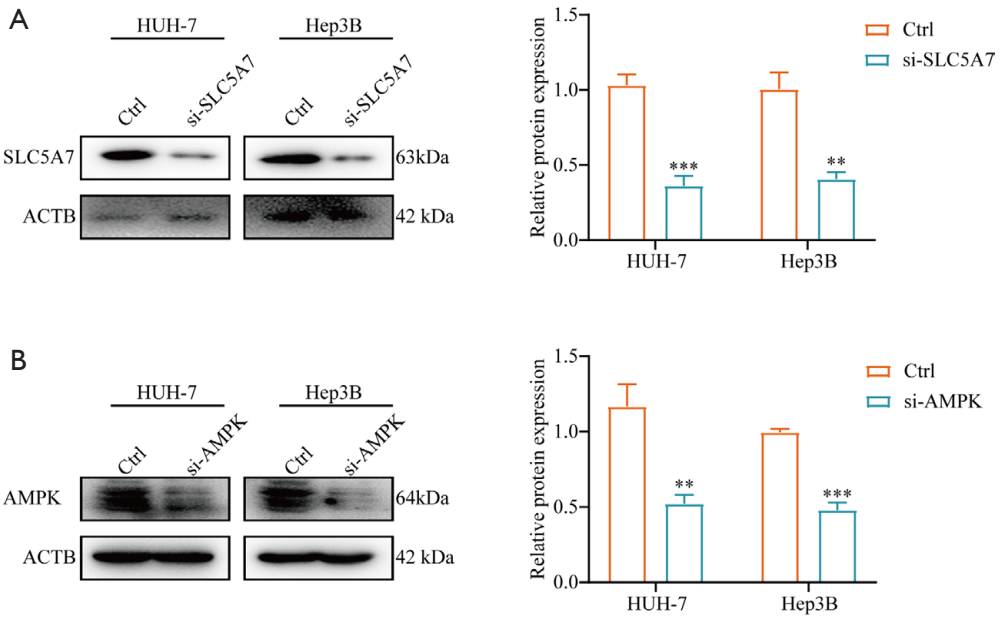

Figure S1 WB assay was used to measure the effect of choline on the expression of SLC5A7 and AMPK, quantitated by optical density and normalized to ACTB levels of the same lane. * choline group *vs.* control group; **P<0.01, ***P<0.001.

Table S1 si-SLC5A7 and si-AMPK sequences

siRNA		Sequence
Scrambled	Sense	5'-UUCUCCGAACGUGUCACGUTT-3'
	Antisense	5'-ACGUGACACGUUCGGAGAATT-3'
si-SLC5A7	Sense	5'- UUAAAGGAGGCAAAAGAAGCG-3'
	Antisense	5'- CUUCUUUUGCCUCCUUUAAAU-3'
Scrambled	Sense	5'-UUCUCCGAACGUGUCACGUTT-3'
	Antisense	5'-ACGUGACACGUUCGGAGAATT-3'
si-AMPK	Sense	5'- CCAUGAAGAGGGCCACAAUTT-3'
	Antisense	5'- AUUGUGGCCCUCUUCAUGGTT-3'

Table S2 The primer sequences

Gene	Primers (5'→3')	GenBank Accession
SLC5A7	Fwd TTGGTGGCCGAGATATTGGTT	NM_60482
	Rev GCCATTGATATACCCTCCTCCG	
18S-rRNA	Fwd GTAACCCGTTGAACCCCATT	NM_544669
	Rev CCATCCAATCGGTAGTAGCG	

https://dx.doi.org/10.21037/hbsn-22-476

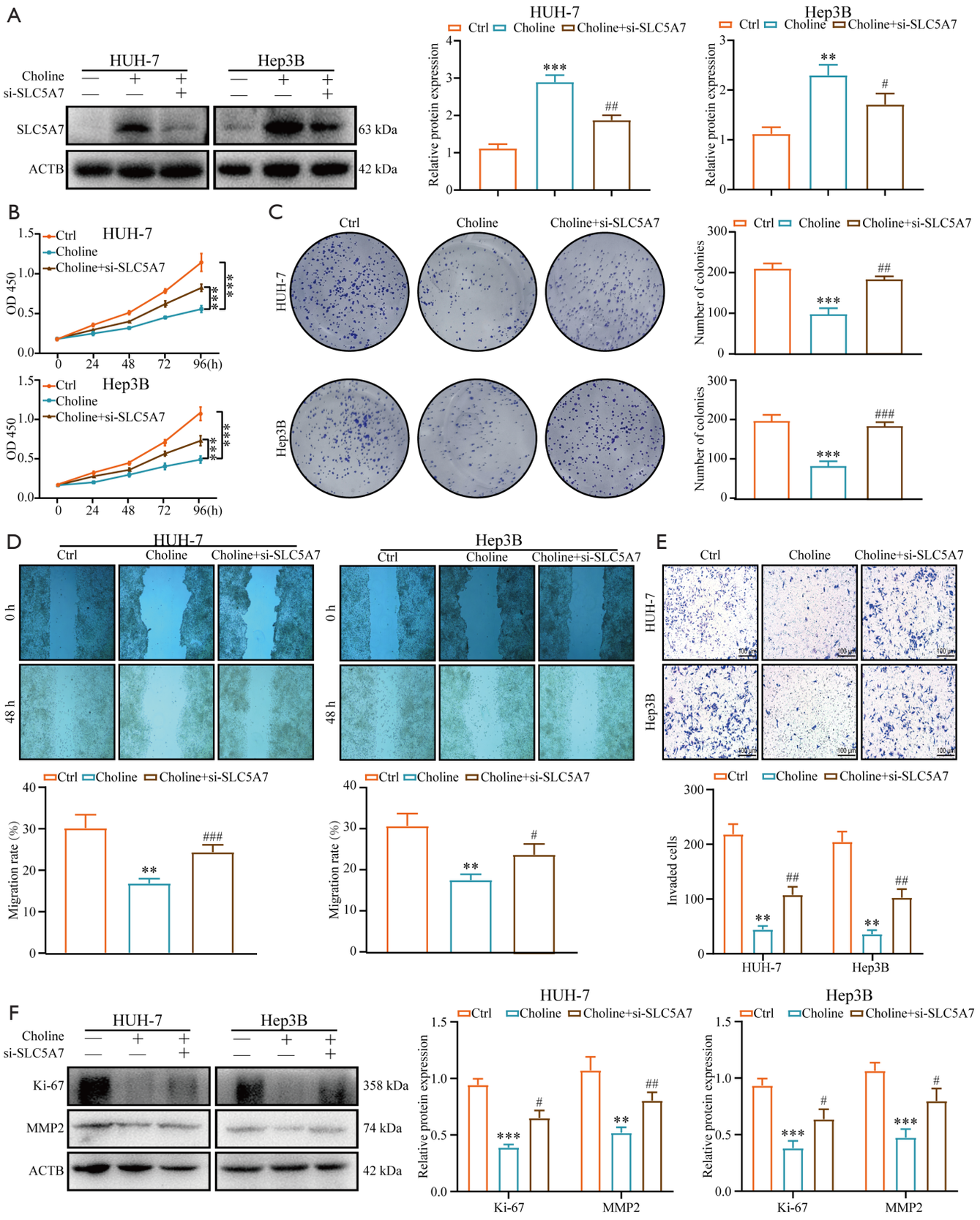

Figure S2 (A) WB analysis of SLC5A7 in HCC cells treated with choline alone and choline combined with si-SLC5A7. Expression of SLC5A7 was quantitated based on optical density. The level of SLC5A7 was normalized to ACTB levels of the same lane. (B,C) HUH-7 and Hep3B cells were subjected to three groups: control group, Choline group, and Choline+si-SLC5A7 group. Cells viability was detected by CCK-8 and colony formation assays. Cells in colony formation assay were stained by 0.1% crystal violet. (D,E) Wound healing and transwell assays were used to detect cell migration and invasion under different treatment. Cells in transwell assay were stained by 0.1% crystal violet. Scale bar= 100 μm. (F) WB analysis of Ki-76 and MMP2 in HCC cells treated with choline alone and choline combined with si-SLC5A7. Expression of Ki-67 and MMP2 was quantitated based on optical density. The level of Ki-67, and MMP2 was normalized to ACTB levels of the same lane. * choline group *vs.* control group, # choline+si-SLC5A7 group *vs.* choline group; **P<0.01, ***P<0.001, #P<0.05, ##P<0.01, ###P<0.001.